Applied Energy 350 (2023) 121713

Contents lists available at ScienceDirect

Applied Energy

journal homepage: www.elsevier.com/locate/apenergy

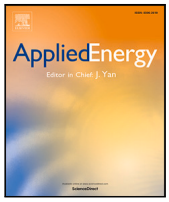

A robust planning model for offshore microgrid considering tidal power and desalination☆

Zhimeng Wang [a], Ang Xuan [a], Xinwei Shen [a,*], Yunfei Du [a], Hongbin Sun [b,c]

[a] Tsinghua Shenzhen International Graduate School (SIGS), Tsinghua University, Shenzhen, 518055, China
[b] Taiyuan University of Technology, Taiyuan, 030002, China
[c] Department of Electrical Engineering, Tsinghua University, Beijing, 100084, China

ARTICLE INFO

Keywords:
Offshore microgrid planning
Column-and-constraint generation algorithm
Two-stage robust optimization
Tidal power
Seawater desalination

ABSTRACT

Increasing attention has been paid to resources on islands, thus microgrids on islands need to be invested. Different from onshore microgrids, offshore microgrids (OM) are usually abundant in ocean renewable energy (ORE), such as offshore wind, tidal power generation (TPG), etc. Moreover, some special loads such as seawater desalination unit (SDU) should be included. In this sense, this paper proposes a planning method for OM to minimize the investment cost while the ORE's fluctuation could be accommodated with robustness. First, a deterministic planning model (DPM) is formulated for the OM with TPG and SDU. A robust planning model (RPM) is then developed considering the uncertainties from both TPG and load demand. The Column-and-constraint generation (C&CG) algorithm is then employed to solve the RPM, producing planning results for the OM that is robust against the worst scenario. Results of the case studies show that the investment and operation decisions of the proposed model are robust, and TPG shows good complementarity with the other RESs.

1. Introduction

Microgrid is a localized, relatively small-scale power system to provide electricity-related services for customers [1], its islanded operation is particularly considered when it comes to remote areas, especially the offshore microgrid (OM), for which undersea cables could be expensive and erratic given the huge distance and complicated environment between the island and the mainland. Meanwhile, distributed energy resources (DERs) are usually incorporated in the microgrids to serve load demands, reduce electricity costs as well as enhance penetration of renewable energy sources (RESs) [2]. The DERs are usually classified as dispatchable units (DUs), nondispatchable units (NDUs), energy storage systems (ESSs), etc. DUs mainly include traditional thermal power generators, which take fossil fuel as an input and could emit toxic gases and generate solid waste, leading to further environmental issues. NDUs are mainly RESs, such as wind power and solar energy. Both DUs and NDUs are generation units, and ESSs are the units serving as reserves by the charging and discharging process.

Till now studies conducted on dealing with diverse uncertainties in microgrids have been investigated, and the optimization methods such as stochastic optimization (SO), distributionally robust optimization (DRO), and robust optimization (RO) have been considered. SO-based microgrid planning methods capture uncertainties based on full information of probabilistic distribution of the underlying uncertainties, while the calculation burden could be huge given the number of scenarios [3–7]. When knowing partial information about the probabilistic distribution of uncertainties, DRO [8] can be applied to deal with uncertainties in power systems [9–11]. However, given that both SO and DRO are based on probabilistic information of uncertainties, they cannot guarantee the security of the microgrid in some extreme/worst cases, which is obviously necessary for OM. The RO, as an optimization method that gives the solution under the worst scenario, has been introduced in lots of problems in the area of energy systems [12–17], and is especially a suitable choice for OM given the reliability of its solution.

Furthermore, several efforts have been made in microgrid planning considering diverse uncertainties using RO. In [18], a bi-level deterministic planning model (DPM) coupled with reserve capacity is proposed, which was further reformulated as a mathematical program with equilibrium constraints and then transformed into a mixed-integer linear programming problem. Literature [19] proposed a probability-weighted RO method, in which uncertainties from both wind power and load demand are captured by probability-weighted uncertainty

☆ This work was supported by National Natural Science Foundation of China (No. 52007123).
* Corresponding author.
E-mail address: xwshen@tsinghua.edu.cn (X. Shen).

https://doi.org/10.1016/j.apenergy.2023.121713
Received 26 May 2023; Received in revised form 18 July 2023; Accepted 2 August 2023
Available online 17 August 2023

Nomenclature

Acronyms

OM	Offshore Microgrid.
DER	Distributed Energy Resource.
RES	Renewable Energy Source.
DU	Dispatchable Unit.
NDU	Nondispatchable Unit.
ESS	Energy Storage System.
RO	Robust Optimization.
SO	Stochastic Optimization.
C&CG	Column-and-Constraint Generation.
DPM	Deterministic Planning Model.
RPM	Robust Planning Model.
ORE	Ocean Renewable Energy.
SDU	Seawater Desalination Unit.
TPG	Tidal Power Generation.

Indices and Set

i, Ω_{DU}	Index and Set for dispatchable units.
j, Ω_{NDU}	Index and Set for traditional nondispatchable units.
k, Ω_{TPG}	Index and Set for tidal generation units.
l, Ω_{ESS}	Index and Set for energy storage systems.
h, H	Index and Set for hour.
d, D	Index and Set for day.
y, Y	Index and Set for year.
$\mathcal{U}$	Uncertainty Set.

Parameters

cc	Annualized investment cost of generating units, $ per MW.
cp	Annualized investment cost of storage (power), $ per MW.
ce	Annualized investment cost of storage (energy), $ per MW.
RP_i, RC_i	Rated power and rated capacity of the ith generation device, MW.
c_i	Levelized operation cost of the ith generation device, $ per MWh.
dr	Discount rate, dimensionless.
κ_y	Coefficient of present-worth value of the yth year, dimensionless.
ν	Punishment for load shedding, dimensionless.
$L^{\max}$	Maximal predicted load demand, MW.
$\tilde{L}_{h,d,y}$	Predicted electricity load demand at hour h, day d, year y, MW.
$\overline{L}, \underline{L}$	Upper and lower deviation of electricity load demand, respectively, MW.
RC_F	Rated capacity of the seawater desalination unit, t.
cc_F	Annualized investment cost of desalination unit, $.
c_F	Annualized operation cost of desalination unit, $ per t.
α_F	Fresh water-electricity conversion efficiency, MW per t.
F_0	Daily fresh water demand, t.
η_l^{ESS}	Efficiency of charging and discharging of the lth ESS, dimensionless.
η_k^{TPG}	Efficiency of the kth tidal generation unit, dimensionless.
$\tilde{P}_{j,h,d,y}$	Nominal generation of the jth RES and the kth TPG unit given the natural condition at hour h, day d, year y, respectively, MW.
$\Gamma_y^L, \Gamma_y^{TPG}$	Uncertainty budget of electricity load demand and tidal power generation in year y, respectively, dimensionless.
β_L, β_{TPG}	Deviation coefficient of load demand and tidal height, respectively, dimensionless.
$\gamma_t^L, \gamma_t^{TPG}$	Uncertainty budget coefficients of load demand and tidal height, respectively, dimensionless.
g	Acceleration due to the Earth's gravity, m/s^2.
ρ	Density of sea water, kg/m^3.
$h_{h,d,y}^{TPG}$	Tidal height at hour h, day d, year y, m.
A_k	Area of the kth tidal generation unit, m^2.

Variables

x_i	Binary decision variable of the investment status of the ith unit, dimensionless.
$P_{i,h,d,y}$	Generation of the ith device at hour h, day d, year y, MW.
$P_{l,h,d,y}^{dch}, P_{i,h,d,y}^{ch}$	Discharging and charging power of the lth energy storage system at hour h, day d, year y, MW.
$F_{h,d,y}$	Amount of fresh water produced by the desalination unit, t.
$SOC_{l,h,d,y}$	State of charge of the ith energy storage system at hour h, day d, year y, MWh.
$LS_{h,d,y}$	Load shedding at hour h, day d, year y, MW.
$L_{h,d,y}$	Electricity load demand at hour b, day h, year t, MW.
$\overline{u}_{h,d,y}^L, \underline{u}_{h,d,y}^L$	Binary decision variables determining whether load demand at hour h, day d, year y should be set as its upper or lower bound, respectively, dimensionless.
$\overline{u}_{h,d,y}^{TPG}, \underline{u}_{h,d,y}^{TPG}$	Binary decision variables determining whether tidal power generation at hour b, day h, year t should be set as its upper or lower bound, respectively, dimensionless.

sets, and the model is solved by a modified column-and-constraint generation (C&CG) algorithm [20]. In [21], Khodaei et al. considered uncertainties from load demand, RES generation and electricity market prices in an interval-based manner and solved the model with Benders decomposition; differently, uncertainties in [22], including RES generation and ambient temperature are solved with C&CG. Similarly, the model in [23] was also solved with C&CG with the uncertainty set formulated as a polyhedron. The nested C&CG algorithm is utilized in [24] to solve the proposed robust planning model (RPM), where uncertainties from RES generation as well as operating states of the bidirectional converters are modeled with interval-partitioned uncertainty sets that reduce the conservativeness of traditional single-interval uncertainty

based robust models. In [25], a robust model was established with uncertainties from load demand and RES generation analyzed with the interval analysis method, and the uncertain constraints are converted to deterministic ones so that the model can be solved easily.

However, none of the above research considered the new elements in OM specifically, such as ocean renewable energy (ORE) including tidal power and wave energy etc, and some special load such as seawater desalination units (SDU). ORE should not be ignored for OM planning, given the abundant quantity of ORE on islands, as well as the uniqueness of OM. Among all types of ORE, tidal power is one of the most promising. Generally, tidal power is caused by periodic changes in sea levels resulting from the gravitational attraction between celestial bodies [26]. Tidal power has some favorable advantages over traditional RESs, such as wind and solar energy, since it is easier to be predicted with decent accuracy many years in advance [27], making it an appropriate choice for planning. Besides, tidal power is expected to have a great potential of 3.6 TW in 2030 [28], which could be highly helpful in enhancing renewable penetration as well as achieving dual carbon goals. Moreover, load of SDU should also be taken into consideration. The importance of fresh water for human beings is needless to say, and islands are especially in shortage of fresh water since they are surrounded by ocean. For island citizens to get fresh water, two methods are feasible: transporting fresh water from mainland, or desalination. Given the distance between mainland and the island, sea water desalination becomes a more economical way. Power consumption of SDU is a unique load for offshore microgrid. Power consumption of SDU could account for as much as around 17% of the total predicted electricity load demand, which is a proportion that should not be ignored. However, few studies incorporating tidal power into OM planning or taking load demand of SDU into consideration have been conducted till now.

The main contributions of this paper are summarized as follows:

(1) A two-stage RPM for OM integrated with SDU and tidal power generation (TPG) is proposed. The first stage includes the investment decisions on various DUs and NDUs, as well as ESSs, while in the second stage the operation decisions are also made considering the uncertainties of both load and tidal generation.
(2) To analyze the role of TPG in OM accurately, its uncertainty is modeled in terms of tidal height, and scenarios with different tidal delays are also simulated. The case studies show the effectiveness of the proposed uncertainty modeling for TPG. It is also shown that, TPG could work complementarily with the other generation methods.
(3) The C&CG algorithm is then employed to solve the two-stage RPM. Numerical experiments in different scenarios show the essential role of ORE in OM planning, and the robustness of the planning results.

The remainder of the paper is organized as follows. Section 2 gives the framework of the planning problem and method. Section 3 introduces the proposed mathematical model, including the objective functions, the constraints and uncertainty modeling of the OM with tidal power in detail. Section 4 provides numerical simulations based on the test microgrid cases. Section 5 summarizes the results and concludes the paper.

2. Framework of the OM planning method

In this paper, the planning problem of an OM is considered. It is assumed that the candidate units of the microgrid include diesel generators (DU), wind turbines, photovoltaics (PV), energy storage systems (ESS) as well as tidal generators, as illustrated in Fig. 1. DSU, as the only device that is able to produce fresh water, will be invested compulsively and is hence not assumed as one of the candidate units.

All the decision variables can be divided into two categories:

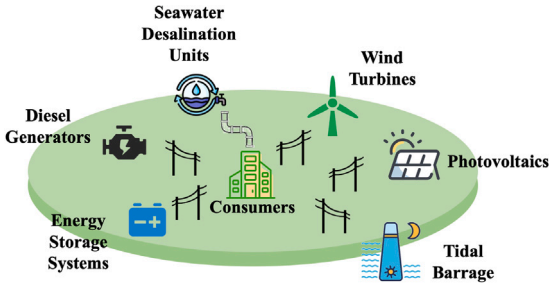

Fig. 1. Structure of the OM discussed in this paper.

(1) Binary decision variables marked with red in Fig. 2, including $x_i, \forall i \in \Omega_{DU}$, $x_j, \forall j \in \Omega_{NDU}$, $x_k, \forall k \in \Omega_{TPG}$, $x_l, \forall l \in \Omega_{ESS}$, for investment decisions of the candidate units, and $\underline{u}^{L}_{h,d,y}$, $\overline{u}^{L}_{h,d,y}$, $\underline{u}^{TPG}_{h,d,y}$, $\overline{u}^{TPG}_{h,d,y}$ for uncertainty decisions. For simplicity, the aforementioned x_i, x_j, x_k, x_l and $\underline{u}^{L}_{h,d,y}$, $\overline{u}^{L}_{h,d,y}$, $\underline{u}^{TPG}_{h,d,y}$, $\overline{u}^{TPG}_{h,d,y}$ are represented by x and u respectively in Fig. 2 and the rest of the paper;

(2) Continuous decision variables marked with blue in Fig. 2, representing power generation quantity of the generation units $P_{i,h,d,y}, \forall i \in \Omega_{DU}$, $P_{j,h,d,y}, \forall j \in \Omega_{NDU}$, $P_{k,h,d,y}, \forall k \in \Omega_{TPG}$, charging and discharging power of the ESSs $P^{ch}_{l,h,d,y}$, $P^{dch}_{l,h,d,y}, \forall l \in \Omega_{ESS}$, as well as fresh water production of the SDU $F_{h,d,y}$. For simplicity, the aforementioned $P_{i,h,d,y}$, $P_{j,h,d,y}$, $P_{k,h,d,y}$, $P^{ch}_{l,h,d,y}$, $P^{dch}_{l,h,d,y}$ and $F_{h,d,y}$ are represented by P and F in Fig. 2 and the rest of the paper.

The inputs of the proposed OM planning model comprise the predicted data of load demand, wind speed, solar radiation and tidal height, the device parameters, and the parameters related to uncertainty modeling of deviation coefficients, uncertainty budget coefficients, delay of tidal height, etc.

The solution procedure is composed of two stages. Investment decisions are made in the first stage, also known as the planning stage. The second stage is known as the operation stage, where the operation strategy in the worst scenario could be derived from the investment decisions determined in the first stage. If investment decisions from the first stage bring infeasibility to the second stage, cuts will be formed and returned to the first stage as additional constraints, where the investment decisions will be optimized again until the optimization problem in the second stage is feasible. Therefore, the outputs of the model include first-stage investment decisions and second-stage operation strategies. The framework of the planning-operation co-optimization model discussed in this paper is illustrated in Fig. 2.

3. Model formulation

In this section, a DPM for the OM, i.e., a model without consideration of uncertainties, is proposed first. Uncertainties are then modeled and the uncertainty sets are formulated, which are then integrated into the original model to derive the robust model.

3.1. Deterministic planning model

3.1.1. Objective function

The objective function (1) of the DPM includes investment cost C^{inv} for capital expenditure of the devices, and operation cost C^{ope} for the real-time scheduling of the microgrid. The object is to minimize the total cost to make the most economical decisions.

$$\min \quad C^{total} = C^{inv} + C^{ope} \tag{1}$$

$$C^{inv} = \sum_{y} \kappa_y \begin{bmatrix} \sum_{i\in\Omega_{DU}} cc_i RC_i x_i \\ + \sum_{j\in\Omega_{NDU}} cc_j RC_j x_j \\ + \sum_{k\in\Omega_{TPG}} cc_k RC_k x_k \\ + \sum_{l\in\Omega_{ESS}} \left(cp_l RP_l + ce_l RC_l\right) x_l \end{bmatrix} \tag{2}$$

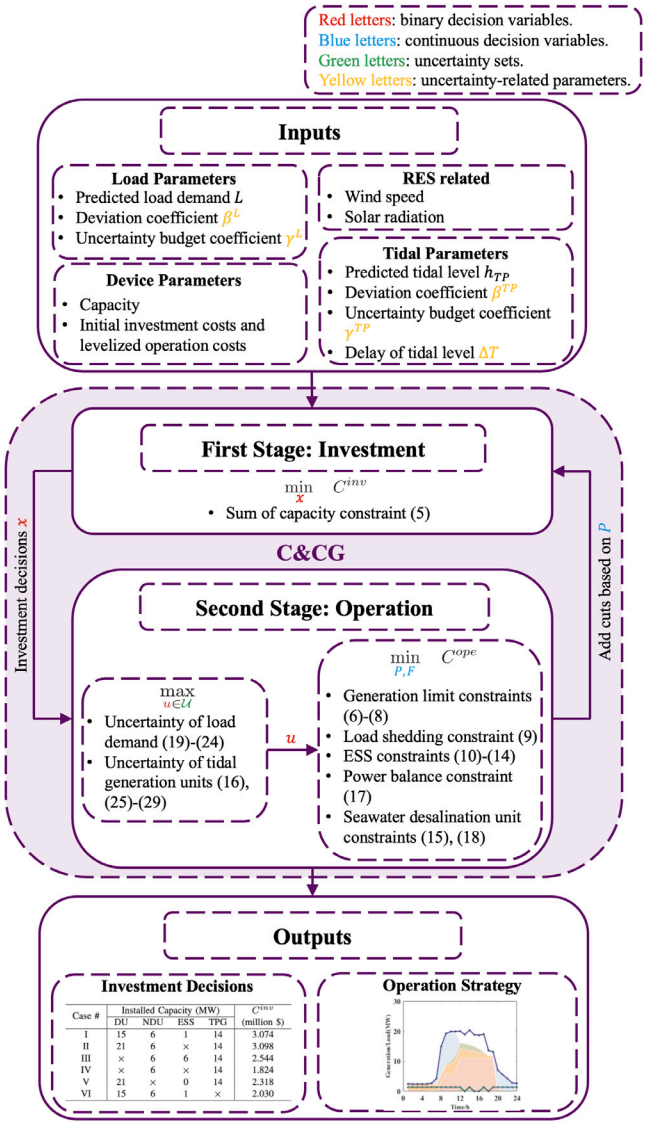

Case #	Installed Capacity (MW)				C^{inv}
	DU	NDU	ESS	TPG	(million $)
I	15	6	1	14	3.074
II	21	6	×	14	3.098
III	×	6	6	14	2.544
IV	×	6	×	14	1.824
V	21	×	0	14	2.318
VI	15	6	1	×	2.030

Fig. 2. Framework of the planning problem discussed in this paper.

where the first three terms in (2) stand for investment costs of DUs, NDUs and TPG units, and the fourth term stands for investment costs of the ESSs. x is the binary decision variable for the device, $x = 1$ indicates that the device is selected to be invested, $x = 0$ otherwise. cc is the annualized investment cost of the device per MW, and RC is the rated capacity of the corresponding device. The investment cost of the lth ESS is formulated as the combination of the cost for rated power RP_l and rated capacity RC_l (here unit: MWh).

Note that there is a coefficient of the present-worth value of the yth year κ_y in C^{inv} so as to count for the effect of the discount rate dr. κ_y can be calculated based on discount rate dr as follows:

$$\kappa_y = \frac{1}{(1+dr)^{y-1}}, \forall y \tag{3}$$

The total operation cost C^{ope} is formed as follows:

$$C^{ope} = \sum_y \sum_d \sum_h \begin{bmatrix} \sum_{i\in\Omega_{DU}} c_i P_{i,h,d,y} \\ +\sum_{k\in\Omega_{TPG}} c_k P_{k,h,d,y} \\ +c_F F_{h,d,y} + \nu LS_{h,d,y} \end{bmatrix}, \forall h,d,y \tag{4}$$

where the first two terms represent the operation costs of DUs and TPG, calculated as the product of the levelized operation cost c and the real-time operation power $P_{h,d,y}$. The third term is the operation cost of SDU, where c_F is the levelized operation cost of SDU, i.e., the operation cost of producing each ton of fresh water, and $F_{h,d,y}$ is the amount of fresh water produced at each time period. The last term is punishment for load shedding, calculated as the product of the punishment factor $\nu_{h,d,y}$ and the shedding-load power $LS_{h,d,y}$. The punishment factor ν for load shedding, also known as the value of lost load, is set as a sufficiently large number so as to drive load shedding to zero.

3.1.2. Constraints

The constraints considered in the DPM of the OM planning problem are as follows:

$$L^{\max} \le \sum_i RP_i x_i + \sum_j RP_j x_j + \sum_k RP_k x_k \tag{5}$$

$$0 \le P_{i,h,d,y} \le RP_i x_i \tag{6}$$

$$0 \le P_{j,h,d,y} \le RP_j x_j \tag{7}$$

$$0 \le P_{k,h,d,y} \le RP_k x_k \tag{8}$$

$$0 \le LS_{h,d,y} \le L_{h,d,y} \tag{9}$$

$$0 \le P^{dch}_{l,h,d,y} \le RP_l x_l \tag{10}$$

$$0 \le P^{ch}_{l,h,d,y} \le RP_l x_l \tag{11}$$

$$SOC_{l,h+1,d,y} = SOC_{l,h,d,y} + P^{ch}_{l,h,d,y}\eta^{ESS}_l - P^{dch}_{l,h,d,y}/\eta^{ESS}_l \tag{12}$$

$$0 \le SOC_{l,h,d,y} \le RC_l x_l \tag{13}$$

$$SOC_{l,1,d,y} = SOC_{l,24,d,y} \tag{14}$$

$$0 \le F_{h,d,y} \le RC_F \tag{15}$$

$$\tilde{P}^{TPG}_{k,h,d,y} = \frac{1}{2}\cdot\rho\cdot g\cdot h^{TPG2}_{h,d,y}\cdot A_k\cdot\eta^{TPG}_k/3600, \quad \forall k\in\Omega_{TPG} \tag{16}$$

$$\sum_i P_{i,h,d,y} + \sum_j P_{j,h,d,y} + \sum_k P_{k,h,d,y} + \sum_l \left(P^{dch}_{l,h,d,y} - P^{ch}_{l,h,d,y}\right) = L_{h,d,y} + \alpha_F F_{h,d,y} - LS_{h,d,y} \tag{17}$$

$$\sum_h F_{h,d,y} \ge F_0 \tag{18}$$

$$\forall i\in\Omega_{DU}, \quad \forall j\in\Omega_{NDU}, \quad \forall k\in\Omega_{TPG}, \quad \forall l\in\Omega_{ESS}, \quad \forall h,d,y$$

All the x are binary decision variables of investment states of the DERs, $x = 1$ indicates the device should be invested and $x = 0$ otherwise. Constraint (5) guarantees the sum of the capacities of all the installed units is higher than the maximal predicted load demand $L^{\max}$ to guarantee the feasibility of the planning problem. Constraint (6) is a capacity limit constraint, ensuring the generation of each DU is no greater than the rated power of the corresponding unit when installed, and is exactly 0 when not installed. The next two constraints, (7) and (8) are formulated in a similar manner, imposing restrictions on the generation of RESs including wind power, solar energy and tidal power. Constraint (9) is to limit load shedding $LS_{h,d,y}$ in the range between 0 and load demand $L_{h,d,y}$ at the moment to guarantee the load shedding is no higher than the load demand. Charging power $P^{ch}_{l,h,d,y}$ and discharging power $P^{dch}_{l,h,d,y}$ of the ESSs are restricted by (10) and (11) in the range between 0 and RP_l of the corresponding unit. Equality constraint (12) is utilized to calculate the state of charge (SOC) of the ESSs. The SOC of each ESS at each time period $SOC_{l,h+1,d,y}$ is calculated based on the last time period $SOC_{l,h,d,y}$ by appending a term related to the charging power of the last time period $P^{ch}_{l,h,d,y}$ and subtracting a term

related to the discharging power of the last time period $P^{dch}_{l,h,d,y}$. Note that efficiencies of the ESSs η^{ESS}_{l} are considered here to account for the fact that not all the power being charged or discharged can be received on the other end perfectly. In (16), generation of a tidal barrage in an hour can be calculated from tidal height [29], where ρ is density of sea water, g is acceleration due to the Earth's gravity, h_{TPG} is tidal height, A_i and η^{TPG}_{k} are the area and efficiency of the kth tidal generation unit, respectively. SOC of each ESS is restricted within the range of its rated capacity by (13), and the SOC of each device at the start of the day $SOC_{l,h,d,y}$ is required to be the same as the value at the end of the day $SOC_{l,H,d,y}$ as required by (14), which is helpful to extend battery life, and helps to ensure that the ESSs can always be utilized when being needed. Power balance is guaranteed in (17), where sum of generation of all the generating units is required to be equal to sum of predicted load demand and load demand from SDU, denoted by $\alpha_F F_{h,d,y}$, where α_F is the fresh water-electricity conversion efficiency, i.e., the amount of power needed to produce each ton of fresh water. Efficiencies of the ESSs are not included here since they are already considered when calculating SOC. In (18), fresh water production in each day is required to meet the daily fresh water demand F_0. Since the storage of fresh water is generally large and simple [30], fresh water demand balance is considered on a daily basis, rather than in each hour.

To conclude, the DPM of the OM can be summarized in the following compact form:

$$\min_{x,P,LS,F} \quad C^{total}$$

$$s.t. \quad \text{Constraints (5)–(18).}$$

3.2. Uncertainty characterization in offshore microgrid

Uncertainties from load demand and tidal generation are formulated in this part.

3.2.1. Load demand uncertainty modeling

The uncertainty set of load demand $\mathcal{U}_L$ is formulated as follows:

$$\mathcal{U}_L : L_{h,d,y} = \tilde{L}_{h,d,y} - \underline{L}_{h,d,y}\underline{u}^{L}_{h,d,y} + \overline{L}_{h,d,y}\overline{u}^{L}_{h,d,y} \tag{19}$$

$$\underline{u}^{L}_{h,d,y} + \overline{u}^{L}_{h,d,y} \le 1 \tag{20}$$

$$\overline{L}_{h,d,y} = \underline{L}_{h,d,y} = \beta_L \tilde{L}_{h,d,y} \tag{21}$$

$$\sum_{d}\sum_{h}\left(\underline{u}^{L}_{h,d,y} + \overline{u}^{L}_{h,d,y}\right) \le \Gamma^{L}_{y} \tag{22}$$

$$\Gamma^{L}_{y} = \gamma^{L}_{y} \cdot D \cdot H \tag{23}$$

$$\forall h, d, y$$

where $\overline{u}^{L}_{h,d,y}$ and $\underline{u}^{L}_{h,d,y}$ are binary decision variables indicating whether the load is increased to its upper limit or decreased to its lower limit, respectively. Constraint (20) guarantees the two binary decision variables will not be set as 1 at the same time. $\overline{L}_{h,d,y}$ and $\underline{L}_{h,d,y}$ are the upper and lower deviation of the uncertainty set, respectively, and can be calculated by (21). In (21), β_L is the deviation coefficient of load demand, and is a positive constant less than 1. Constraint (19) can be further elaborated as follows:

$$L_{h,d,y} = \begin{cases} \tilde{L}_{h,d,y} - \underline{L}_{h,d,y}, \text{ if } \underline{u}^{L}_{h,d,y} = 1, \overline{u}^{L}_{h,d,y} = 0 \\ \tilde{L}_{h,d,y} + \overline{L}_{h,d,y}, \text{ if } \underline{u}^{L}_{h,d,y} = 0, \overline{u}^{L}_{h,d,y} = 1 \\ \tilde{L}_{h,d,y}, \text{ if } \underline{u}^{L}_{h,d,y} = 0, \overline{u}^{L}_{h,d,y} = 0 \end{cases} \tag{24}$$

hence when $\underline{u}^{L}_{h,d,y} = 1$ and $\overline{u}^{L}_{h,d,y} = 0$, a lower deviation is subtracted from the predicted value, and when $\overline{u}^{L}_{h,d,y} = 1$ and $\underline{u}^{L}_{h,d,y} = 0$, an upper deviation is added to the predicted value. When both of them are 0, the predicted value of load demand is achieved. Constraint (22) sets an uncertainty budget Γ^{L}_{y} for the uncertainty set [31], restricting the number of deviations of all time periods in one year in which the load demand is far away from its predicted value, hence this parameter helps to adjust the conservatism of the model. Γ^{L}_{y} can be calculated from (23), and it is the coefficient controlling the percentage of the deviated scenarios, and γ^{L}_{y} is within the range of $[0, 1]$. For instance, when $\gamma^{L}_{y} = \Gamma^{L}_{y} = 0$, load demands in all time periods are assumed as the corresponding predicted values, thus, there is no robustness considered, and the model is deterministic. When setting γ^{L}_{y} as a higher value, Γ^{L}_{y} also goes up and a higher degree of robustness is achieved and the model is more conservative. Adjusting the uncertainty budget helps to adjust the extent to which uncertainty is considered. A higher uncertainty budget allows more deviation points, a higher degree of uncertainty is thus achieved and vice versa.

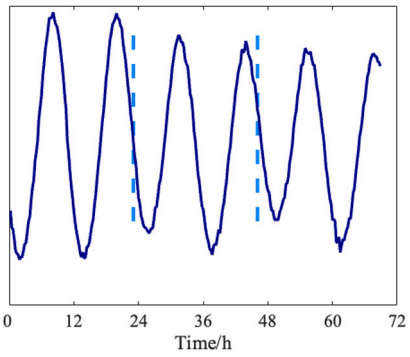

Fig. 3. Typical tidal heights in consecutively three days.

3.2.2. Tidal power uncertainty modeling

Tides are generally semidiurnal, with two high tides and two low tides per day, with two high tides located at 4:00–11:00 am and 4:00–11:00 pm, respectively, as shown in Fig. 3.

Since the effect of tidal heights can be reflected in TPG as in (16), uncertainty of tidal heights is formed as an interval-based set of TPG in a similar manner as follows:

$$\mathcal{U}_{TPG} : P^{TPG}_{k,h,d,y} = \tilde{P}^{TPG}_{k,h,d,y} - \underline{P}^{TPG}_{k,h,d,y}\underline{u}^{TPG}_{k,h,d,y} + \overline{P}^{TPG}_{k,h,d,y}\overline{u}^{TPG}_{k,h,d,y} \tag{25}$$

$$\underline{u}^{TPG}_{k,h,d,y} + \overline{u}^{TPG}_{k,h,d,y} \le 1 \tag{26}$$

$$\overline{P}^{TPG}_{k,h,d,y} = \underline{P}^{TPG}_{k,h,d,y} = \beta_{TPG}\tilde{P}^{TPG}_{k,h,d,y} \tag{27}$$

$$\sum_{d}\sum_{h}\left(\underline{u}^{TPG}_{k,h,d,y} + \overline{u}^{TPG}_{k,h,d,y}\right) \le \Gamma^{TPG}_{y} \tag{28}$$

$$\Gamma^{TPG}_{y} = \gamma^{TPG}_{y} \cdot D \cdot H \tag{29}$$

$$\forall k \in \Omega_{TPG}, \forall h, d, y$$

Besides, time of peak of tidal level is also assumed as uncertain and the time delay ΔT is assumed to be ± 4 h within the predicted time. $\Delta T > 0$ corresponds to the case of the peaks coming earlier and $\Delta T < 0$ otherwise. When $\Delta T = 0$, the predicted time of peaks is assumed to be achieved. When the predicted levels are moved forward or backward, the vacated points are filled with 0, as illustrated in Fig. 4. Scenarios with different ΔT are simulated and analyzed in the case studies.

3.3. Robust planning model for offshore microgrid

A two-stage RPM can be established considering the uncertainties of load demand and tidal generation. In the first stage, the investment status of the units are determined by a master problem to minimize the investment cost, assuming load demand and tidal generation follow

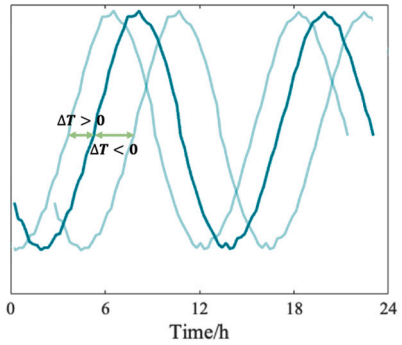

Fig. 4. Modeling of uncertainty time of peaks of tidal heights.

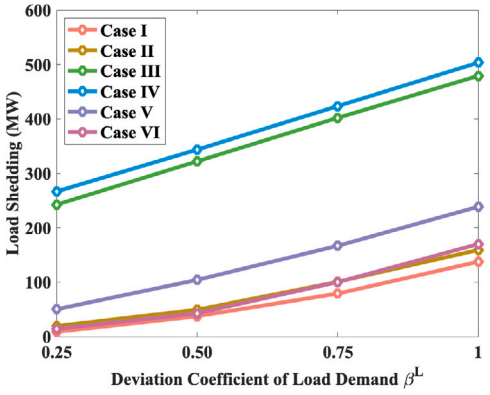

Fig. 5. Load shedding of the RPM with different β^L given investment decisions of the DPM.

the predicted values. After achieving the worst case, the operation strategies are determined in the second stage of the model to minimize the operation cost given the worst case. The derived model is as follows:

$$\min_{x} \quad C^{inv} + \max_{u} \min_{P,LS,F} \quad C^{ope}$$

$$s.t. \quad \text{Constraints (5)–(23), (16)–(29).}$$

where $\mathcal{U} = \mathcal{U}_L \cup \mathcal{U}_{TPG}$ is the union of the considered uncertainty sets. The two-stage RPM is solved using C&CG algorithm [20], which shows better computational efficiency in terms of convergence speed and time compared with Benders Decomposition [20,32].

4. Case studies

Numerical cases are tested in this section. The basic parameters of the test system are introduced first, followed by the results and analyses of the numerical simulations under different conditions.

The candidate devices include six DUs, two NDUs, three ESSs and four TPG units. The fixed parameters of the candidate units are listed in Tables 1–4. The efficiencies of charging and discharging of the ESSs are all assumed as 90%, and the planning horizon is 20 years. Daily fresh water demand is set as 9000 t, and the capacity of SDU is set as 450 t/h. Annualized investment costs and levelized operation costs of the SDU are set as 1.8M $ and 1 $/t. Fresh water-electricity conversion efficiency α_F is 3 kW/t, namely, each ton of fresh water production consumes 3 kW of electricity.

To start with, six DER configuration strategies are designed in Table 5, where ✓and × stand for the corresponding device is allowed and not allowed to be invested, respectively.

Table 1
Parameters of the candidate DUs.

Unit no.	Capacity (MW)	Levelized operation cost ($/MWh)	Annualized investment cost ($/MW)
1	6	140	44,000
2	5	130	54,000
3	4	120	64,000
4	3	110	74,000
5	2	100	84,000
6	1	90	94,000

Table 2
Parameters of the candidate NDUs.

Unit no.	Capacity (MW)	Levelized operation cost ($/MWh)	Annualized investment cost ($/MW)	Type of energy
1	4	–	150,000	WT
2	2	–	90,000	PV

Table 3
Parameters of the candidate ESSs.

Unit no.	Rated power (MW)	Rated energy (MWh)	Annualized investment cost - Power ($/MW)	Annualized investment cost - energy ($/MWh)
1	1	6	60,000	30,000
2	2	6	30,000	30,000
3	3	6	20,000	30,000

Table 4
Parameters of the candidate TPG units.

Unit no.	Capacity (MW)	Levelized operation cost ($/MWh)	Annualized investment cost ($/MW)
1	5	–	54,000
2	4	–	72,000
3	3	–	90,000
4	2	–	108,000

Table 5
Device configuration strategies of test cases.

Case #	DU	NDU	ESS	TPG
I	✓	✓	✓	✓
II	✓	✓	×	✓
III	×	✓	✓	✓
IV	×	✓	×	✓
V	✓	×	✓	✓
VI	✓	✓	✓	×

4.1. Analysis of effectiveness of robust planning

In this section, investment decisions and the corresponding costs of RPM is compared with those of DPM to verify the robustness. Uncertainty budget coefficient γ^L and deviation coefficient of load demand β^L are both set as 0.5 in the RPM. Several scenarios representing different weather and load conditions are simulated. Investment decisions and costs of two typical days are listed in Table 6. Typical day I has lower electricity load demand and less solar radiation, which can be regarded as fall, and typical day II has relatively higher electricity load demand and more solar radiation, which can be regarded as summer. The last column in Table 6 show the quantity of load shedding when implementing the investment decisions from DPM into RPM in the same case. Quantities of load shedding of the opposite scenarios are not listed since there is definitely no load shedding given the more abundant devices determined in the RPM.

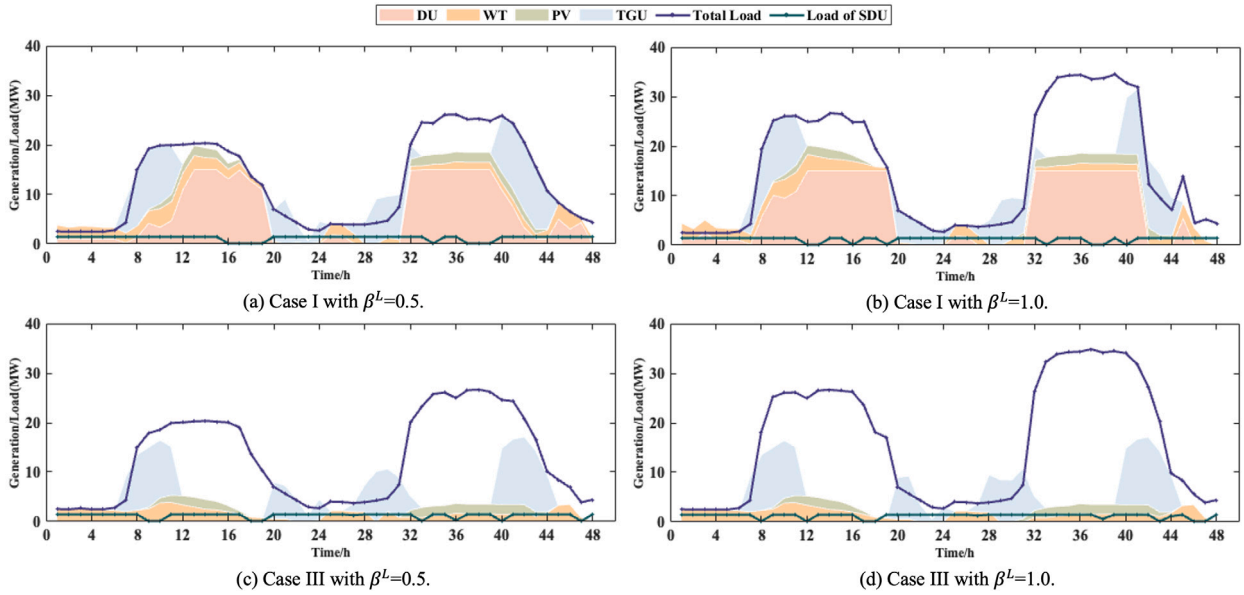

Fig. 6. Scheduling diagrams of cases I and IV with γ^L set as 0.5 and β^L set as 0.5 or 1 in scenario I.

Table 6
Comparison of investment decisions and costs between RPM and DPM under different DER configurations.

Case #		Installed capacity (MW)				C^{inv}	LS
		DU	NDU	ESS	TPG	(M $)	(MW)
I	DPM	15	6	5	14	3.314	37.47
	RPM	21	6	5	14	3.578	
II	DPM	15	6	–	14	2.834	49.31
	RPM	21	6	–	14	3.098	
V	DPM	15	–	6	14	2.774	66.04
	RPM	21	–	6	14	3.038	
VI	DPM	15	6	3	–	2.030	61.51
	RPM	21	6	5	–	2.534	

Table 7
Investment decisions and costs of DPM under different DER configurations.

Case #	Installed capacity (MW)				C^{inv}
	DU	NDU	ESS	TPG	(M $)
I	15	6	5	14	3.314
II	15	6	–	14	2.834
III	–	6	6	14	2.544
IV	–	6	–	14	1.824
V	15	–	6	14	2.774
VI	15	6	3	–	2.030

It is obvious that C^{inv} of RPM under the discussed cases are always higher than those of DPM. Nevertheless, as shown in Table 6, there are more devices invested in all the discussed cases, hence robustness is guaranteed by more devices and more investment. Besides, the installed capacity of DU in all the four discussed cases tends to increase from DPM to RPM, demonstrating DUs' indispensable role in handling uncertainty and enhancing robustness. Also, when implementing investment decisions from DPM into RPM, load demands are curtailed by some amount since the decisions from DPM are not robust enough, being unable to handle the worst scenario in the uncertainty sets, demonstrating the robustness of the RPM.

4.2. Analysis of uncertainty of load demand

In this part, effect of uncertainty from load demand on load shedding is analyzed. To start with, all the uncertainty-related coefficients are set as 0 under the DER configurations of cases I–VI and the investment decisions in these cases are derived and listed in Table 7. The investment decisions are then integrated into the system with β^L varying from 0.25 to 1 and γ^L set as 0.5. The resulting load shedding are plotted in Fig. 5, and scheduling diagrams of cases I and IV with γ^L set as 0.25 or 0.5 are shown in Fig. 6, where the white unfilled parts represent the curtailed load demand.

There is an obvious increasing trend in Fig. 5 as the deviation coefficient of load demand β^L increases from 0.25 to 1. Such a trend is intuitive since a higher β^L leads to higher load demand to be satisfied with consideration of uncertainty, and given the limited ability of the invested devices derived from the deterministic cases, more loads has to be curtailed. Also, load in cases III and IV, i.e., the two cases without investment of DUs, is curtailed by a relatively large quantity as can be found in Fig. 5 as well as Fig. 6(c)(d), demonstrating DUs' significant and reliable role in meeting load demands. By comparing cases III and IV, it is easy to discover that the load shedding of case IV is slightly higher, showing ESSs' contribution in helping to satisfy the loads. However, the contribution is not that significant since ESSs' main function lies in smoothing fluctuation of load demand, but not satisfy the load directly.

It is worth mentioning that SDUs mainly work during the early morning and late evening, just complementary to the time domain distribution of load demand, thus helping ease the load pressure during the peak time and make full use of generation during the other periods of the day. Part of the fresh water is produced during the peaks, when the generation from solar energy is relatively abundant. Such characteristics of the SDUs make full use of lots of the generation methods throughout the day.

4.3. Analysis of uncertainty of tidal generation

In this section, uncertainties of tidal height and time of tidal peak are analyzed. Different values of ΔT, γ^{TPG} and β^{TPG} are simulated and the daily average generation percentage of the simulated scenarios, as shown in Fig. 7, are compared and analyzed. The daily scheduling results are shown in Fig. 8.

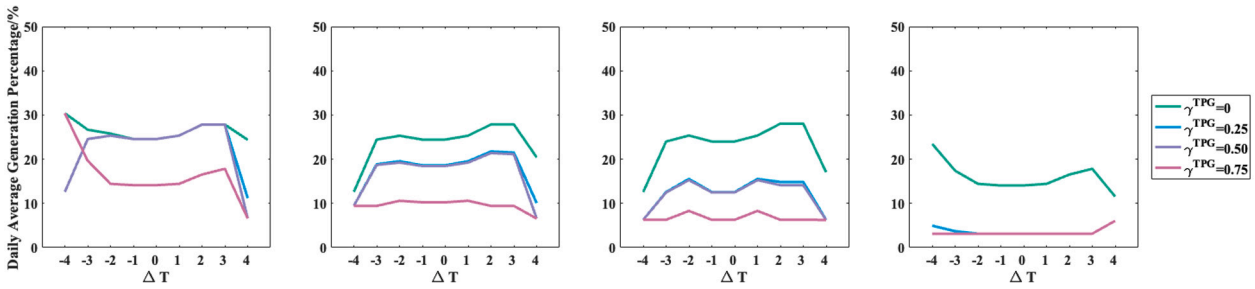

Fig. 7. Daily average generation percentage from TPG in OM with different values of β^{TPG}, γ^{TPG} and ΔT.

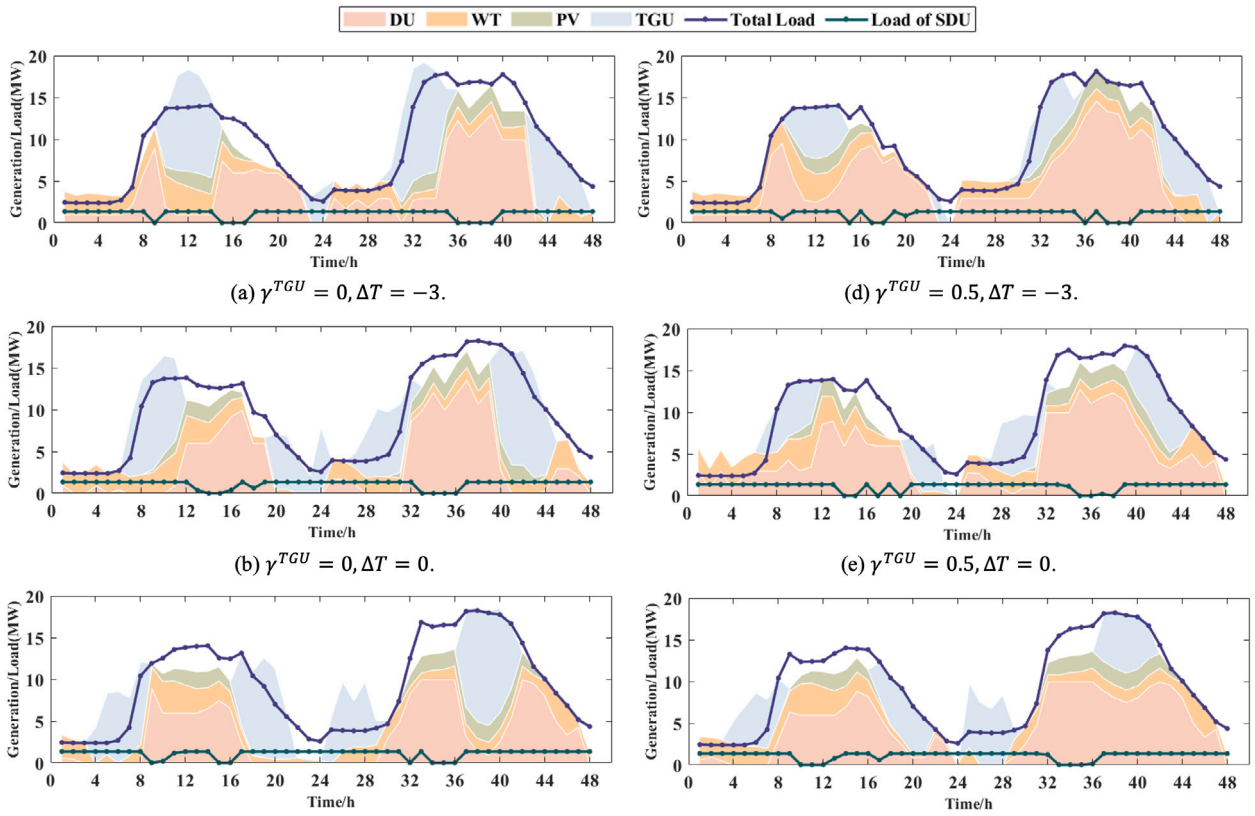

Fig. 8. Scheduling diagrams with β^{TPG} set as 0.5, ΔT set as −3, 0 or +3 and γ^{TPG} set as 0 or 0.5.

It can be discovered that, generally speaking, a higher γ^{TPG} leads to lower generation percentage from TPG, and a higher β^{TPG} shows similar effects. That is because both higher γ^{TPG} and β^{TPG} indicate higher level of uncertainty of TPG, and the worst cases given such parameters lead to lower tidal levels, and thus less power generation from the TPG units, which further lead to lower daily average generation percentage. As can be observed in Fig. 7, due to the high level of uncertainty, there is sometimes even no TPG units invested when γ^{TPG} is set as 0.75 and β^{TPG} set as 0.50 or higher.

In terms of tidal delay, when ΔT is set as around −3 or 3, higher daily average generation percentage can be achieved as shown in Fig. 7. The scheduling diagrams with ΔT set as −3, 0 and 3 and γ^{TPG} set as 0 and 0.50 given a β^{TPG} of 0.50 can be found in Fig. 8. It is obvious that when setting ΔT as −3, most of the generation from TPG lies in the middle of the day, aligning with peak of electricity load demand. While when setting ΔT as +3, generation of TPG shows two peaks, perfectly filling in time when generation from PV is not abundant, hence the complementarity helps to enhance consumption of RESs, especially TPG in this case.

4.4. Analysis of uncertainty from both load demand and tidal height

In this section, uncertainties of load demand and tidal height are considered concurrently, and the resulting investment decisions are analyzed and discussed.

The two uncertainty budget coefficients γ^{L} and γ^{TPG} are both taken from 0 to 0.5 with an interval of 0.25, and the resulting operation costs are illustrated in Fig. 9, where higher costs tend to make the color of the cell darker, and lower costs otherwise. Horizontal and vertical axes in the figure stand for uncertainty budget coefficient of load demand γ^{L} and uncertainty budget coefficient of tidal level γ^{TPG}, respectively.

As can be observed in Fig. 9, both uncertainty budget coefficients give rise to C^{inv}, while γ^{L} contributes more compared with γ^{TPG}. This is caused by the fact that γ^{L} affects the load demand directly, while γ^{TPG} is just a parameter that could affect which DER to generate the power, having less impacts on costs.

Investment decisions of the cases when both γ^{L} and γ^{TPG} are set as 0.5 are listed in Table 8, where - indicates that the corresponding set of device is not allowed to be invested according to the setting of the case.

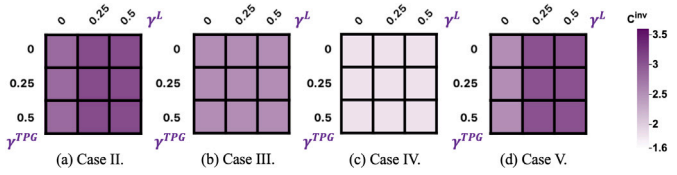

Fig. 9. Investment costs considering different γ^L and γ^{TPG} under different DER configurations.

Table 8
Investment decisions and costs under different DER configurations with $\gamma^L = \gamma^{TPG} = 0.5$.

Case #	Installed capacity (MW)				C^{inv}
	DU	NDU	ESS	TPG	(M $)
II	21	6	–	14	3.098
III	–	6	6	14	2.544
IV	–	6	–	14	1.824
V	21	–	6	14	3.038
VI	21	6	3	–	2.294

5. Conclusion

In this paper, a two-stage robust planning model for offshore microgrid incorporated with modeling of tidal power generation and seawater desalination units is proposed. The uncertainties of load demand and tidal power generation are both modeled and considered. The planning model is solved with the C&CG algorithm. Case studies verify the model's effectiveness and analyze the robustness of different distributed energy resources configuration strategies. Besides, effects of uncertainties are also analyzed.

The simulation results show the function of energy storage systems in peak shaving, helping to move the load peak and smoothen the load curve. Also, the microgrid can also work without traditional dispatchable units, hence a 100% renewable microgrid could be possible. The outputs from tidal generators and PVs show complementarity due to the renewable energy sources' natural characteristics, and the power consumption of seawater desalination units tends to align with the outputs of renewable energy sources. Thus, the combination of them is a valuable part of offshore microgrid planning and worth spreading.

However, the investment costs for tidal generation units are still high compared with traditional dispatchable units, and economic issues could lead to more installations of traditional dispatchable units that are less environmental-friendly. We are looking forward to seeing more developments in tidal power generation units, such as higher energy efficiency and more mature manufacturing, so that the investment costs could be driven down. Lower costs would lead to more investment of these environmental-friendly devices, which are beneficial for the environment while satisfying electricity load demand on the islands.

The future work will focus on considering the connection between several microgrids and developing accelerating solving algorithm for the model.

CRediT authorship contribution statement

Zhimeng Wang: Writing – original draft, Visualization, Validation, Methodology, Investigation, Conceptualization. **Ang Xuan:** Writing – review & editing. **Xinwei Shen:** Writing – review & editing, Supervision. **Yunfei Du:** Writing – review & editing. **Hongbin Sun:** Supervision.

Declaration of competing interest

The authors declare that they have no known competing financial interests or personal relationships that could have appeared to influence the work reported in this paper.

Data availability

Data will be made available on request.

References

[1] Shahidehpour M, Li Z, Bahramirad S, Li Z, Tian W. Networked microgrids: Exploring the possibilities of the IIT-Bronzeville grid. IEEE Power Energy Mag 2017;15(4):63–71.
[2] Shahidehpour M. Role of smart microgrid in a perfect power system. In: IEEE PES general meeting. IEEE; 2010, p. 1.
[3] Su W, Wang J, Roh J. Stochastic energy scheduling in microgrids with intermittent renewable energy resources. IEEE Trans Smart grid 2013;5(4):1876–83.
[4] Narayan A, Ponnambalam K. Risk-averse stochastic programming approach for microgrid planning under uncertainty. Renew energy 2017;101:399–408.
[5] Wu Z, Gu W, Wang R, Yuan X, Liu W. Economic optimal schedule of CHP microgrid system using chance constrained programming and particle swarm optimization. In: 2011 IEEE power and energy society general meeting. IEEE; 2011, p. 1–11.
[6] Wu H, Liu X, Ding M. Dynamic economic dispatch of a microgrid: Mathematical models and solution algorithm. Int J Electr Power Energy Syst 2014;63:336–46.
[7] Mohammadi S, Soleymani S, Mozafari B. Scenario-based stochastic operation management of microgrid including wind, photovoltaic, micro-turbine, fuel cell and energy storage devices. Int J Electr Power Energy Syst 2014;54:525–35.
[8] Bertsimas D, Sim M, Zhang M. Adaptive distributionally robust optimization. Manage Sci 2019;65(2):604–18.
[9] Guevara E, Babonneau F, Homem-de Mello T, Moret S. A machine learning and distributionally robust optimization framework for strategic energy planning under uncertainty. Appl Energy 2020;271:115005.
[10] Lu X, Chan KW, Xia S, Zhou B, Luo X. Security-constrained multiperiod economic dispatch with renewable energy utilizing distributionally robust optimization. IEEE Trans Sustain Energy 2018;10(2):768–79.
[11] Hu C, Liu X, Lu J, Wang C-H. Distributionally robust optimization for power trading of waste-to-energy plants under uncertainty. Appl Energy 2020;276:115509.
[12] Nazari-Heris M, Mohammadi-Ivatloo B. Application of robust optimization method to power system problems. In: Classical and recent aspects of power system optimization. Elsevier; 2018, p. 19–32.
[13] Zhao C, Wang J, Watson J-P, Guan Y. Multi-stage robust unit commitment considering wind and demand response uncertainties. IEEE Trans Power Syst 2013;28(3):2708–17.
[14] Jabr RA. Robust transmission network expansion planning with uncertain renewable generation and loads. IEEE Trans Power Syst 2013;28(4):4558–67.
[15] Rahimiyan M, Baringo L. Strategic bidding for a virtual power plant in the day-ahead and real-time markets: A price-taker robust optimization approach. IEEE Trans Power Syst 2015;31(4):2676–87.
[16] Zhang Y, Gatsis N, Giannakis GB. Robust energy management for microgrids with high-penetration renewables. IEEE Trans Sustain Energy 2013;4(4):944–53.
[17] Martinez-Mares A, Fuerte-Esquivel CR. A robust optimization approach for the interdependency analysis of integrated energy systems considering wind power uncertainty. IEEE Trans Power Syst 2013;28(4):3964–76.
[18] Quashie M, Marnay C, Bouffard F, Joós G. Optimal planning of microgrid power and operating reserve capacity. Appl Energy 2018;210:1229–36.
[19] Zhang C, Xu Y, Dong ZY. Probability-weighted robust optimization for distributed generation planning in microgrids. IEEE Trans Power Syst 2018;33(6):7042–51.
[20] Zeng B, Zhao L. Solving two-stage robust optimization problems using a column-and-constraint generation method. Oper Res Lett 2013;41(5):457–61.
[21] Khodaei A, Bahramirad S, Shahidehpour M. Microgrid planning under uncertainty. IEEE Trans Power Syst 2014;30(5):2417–25.
[22] Tan H, Ren Z, Yan W, Wang Q, Mohamed MA. A wind power accommodation capability assessment method for multi-energy microgrids. IEEE Trans Sustain Energy 2021;12(4):2482–92.
[23] Wang Z, Chen B, Wang J, Kim J, Begovic MM. Robust optimization based optimal DG placement in microgrids. IEEE Trans Smart Grid 2014;5(5):2173–82.
[24] Qiu H, Gu W, Xu Y, Wu Z, Zhou S, Wang J. Interval-partitioned uncertainty constrained robust dispatch for AC/DC hybrid microgrids with uncontrollable renewable generators. IEEE Trans Smart Grid 2018;10(4):4603–14.
[25] Yang D, Jiang C, Cai G, Yang D, Liu X. Interval method based optimal planning of multi-energy microgrid with uncertain renewable generation and demand. Appl Energy 2020;277:115491.
[26] Frau JP. Tidal energy: promising projects: La rance, a successful industrial-scale experiment. IEEE Trans Energy Convers 1993;8(3):552–8.
[27] Khan K, Ahmed SM, Akhter M, Alam R, Hossen M. Wave and tidal power generation. Int J Adv Res Innov Ideas Educ 2018;4(6):71–82.
[28] Sleiti AK. Tidal power technology review with potential applications in gulf stream. Renew Sustain Energy Rev 2017;69:435–41.

[29] Lamb H. Hydrodynamics. Cambridge University Press; 1994, p. 260.
[30] Wang Z, Lin X, Tong N, Li Z, Sun S, Liu C. Optimal planning of a 100% renewable energy island supply system based on the integration of a concentrating solar power plant and desalination units. Int J Electr Power Energy Syst 2020;117:105707.
[31] Bertsimas D, Sim M. The price of robustness. Oper Res 2004;52(1):35–53.
[32] Zhao L, Zeng B. Robust unit commitment problem with demand response and wind energy. In: 2012 IEEE power and energy society general meeting. IEEE; 2012, p. 1–8.